SLAC-TN-04-063
September 2004

Ruthenium-Platinum Thin Film Analysis Using Grazing Incidence X-ray Diffraction

Lindsay E. Jones
Office of Science, SULI Program
Northeastern University, Boston
Stanford Synchrotron Radiation Laboratory
Menlo Park, California

August 21, 2004

Prepared in partial fulfillment of the requirements of the Office of Science, DOE Student Undergraduate Laboratory Internship (SULI) Program under the direction of Michael F. Toney at the Stanford Synchrotron Laboratory at the Stanford Linear Accelerator Center.

Participant: _____
Signature

Research Advisor: _____
Signature

Work supported in part by Department of Energy contract DE-AC02-76SF00515.

Table of Contents

ABSTRACT

Structural Analysis of RuPt samples using Grazing Incidence Angle X-ray Diffraction. LINDSAY E. JONES (Northeastern University, Boston, MA, 02115) MICHAEL F. TONEY (Stanford Synchrotron Radiation Laboratory, Menlo Park, California 94309).

Ruthenium (Ru, Z = 44) is a Platinum Group Metal that has a standard hexagonal close packed (HCP) crystalline structure. Platinum (Pt, Z = 78) has a face-centered cubic (FCC) crystalline structure. When these metals are co-sputtered onto a silicon substrate, creating a few nm-thin film, they form an alloy with a combination of HCP and FCC structure. Direct methanol fuel cells rely on an anode catalyst to draw hydrogen from liquid methanol. Highly efficient fuel cells based on polymer electrolyte catalysts, known as proton-exchange membrane fuel cells, have been developed, but require large amounts of a costly platinum catalyst. Thin-film nanostructure bimetallic alloys have been produced to reduce the amount of expensive Platinum needed for catalysis, and also to improve the electrochemical properties of the catalyst. Supported RuPt particles have been shown to have superior activity as anode catalysts for methanol electro-oxidation and demonstrate an improvement in resistance to poisoning in comparison to unalloyed Pt. The percentage of Ruthenium in a RuPt thin film and the process by which the alloy is produced will dictate the crystalline structure, and thus the electrochemical properties of the film. Pure Ruthenium, Pure Platinum, and eight intermediate samples at differing percent composition of Ruthenium were characterized by their X-ray diffraction patterns. The incident beam is from the Stanford Synchrotron Radiation Laboratory beam and operates at approximately a 1.4 Angstrom wavelength. The results show that 0% Ru through 46.17% Ru exhibit a majority FCC structure, 56.07% Ru and 60.61% Ru are mixed phase, and from 67.03% Ru through 100% Ru, the samples exhibit a HCP structure.

INTRODUCTION

Ruthenium (Ru, Z = 44) is a Platinum Group Metal that has a standard hexagonal close packed (HCP) crystalline structure. Platinum (Pt, Z = 78) has a face-centered cubic (FCC) crystalline structure [13]. When these metals are co-sputtered onto a silicon substrate, creating a few nm-thin film, they form an alloy with a combination of HCP and FCC structure [7]. Nanostructure materials are of interest due to their unique catalytic, physical, electrochemical properties, electronic, and optical properties, which differ greatly from the same particles in the bulk state [1, 4, 6, 8-9].

One application for these thin films of bimetallic alloy is as a catalyst for a Direct Methanol Fuel Cell (DMFC). These have attracted interest because they have the potential for low operating temperatures, easy handling, the use of high energy density methanol, and developing micro-sized fuel cells [1, 8, 10]. Electrochemical fuel cells convert the chemical energy of fuels directly into electrical energy to provide a clean and highly efficient source of electrical energy. In the DMFC, the anode catalyst itself draws the hydrogen from the liquid methanol. Efficiencies of about 40% are expected [13]. Highly efficient fuel cells based on polymer electrolyte catalysts, known as proton-exchange membrane fuel cells, have been developed, but require large amounts of a costly platinum catalyst. Thin-film nanostructure bimetallic alloys have been produced to reduce the amount of expensive Platinum needed for catalysis, and also to improve the electrochemical properties of the catalyst used [12, 16]. Supported RuPt particles have been shown to have superior activity as anode catalysts for methanol electrooxidation and demonstrate a marked improvement in resistance to CO poisoning in comparison to unalloyed Pt. The poisoned Platinum can be regenerated via the reaction of surface CO with oxygen species associated with an element such as ruthenium to yield CO_2 [1,3, 15]. Very common support materials for the thin films are carbon, alumina and silica. It

appears that the best catalysts will be those that maximize the content of Ru in the FCC Pt phase [2], but unambiguous proof of this is lacking.

The percentage of Ruthenium in a RuPt sample and the process by which the alloy is produced will dictate the crystalline structure, and thus the physical and chemical properties of the film. Pure Ru, pure Pt, and eight samples of RuPt in differing combinations will be structurally analyzed. By examining the peaks in X-ray diffraction patterns of all samples (whose percent compositions are known), one will be able to determine the effect of the percentage of Ru on the crystalline structure.

MATERIALS AND METHODS

The samples were prepared by Kyung-Won Park and Yung-Eun Sung of the Research Center for Energy Conversion and Storage at Seoul National University in Seoul, Korea, by a co-sputtering method [11]. In the diffraction measurements, the sample is held to a Huber diffractometer by way of a vacuum chuck, and it is surrounded by a Helium environment to reduce unnecessary scattering of x-rays from the air near the sample. The beam, upon entering the radiation hutch, passes through evacuated flight tubes, an ion chamber, and beam defining slits. After grazing the sample, the diffracted beams pass through Soller slits, used to define the scattering angle, before reaching the detector. Using SUPER, a data collection and motor control program developed by Sean Brennan of SSRL, diffraction patterns were obtained. We ran 10 samples through a battery of scans. The samples are denoted: Pure Ru, ~ 90% Ru, ~ 80% Ru, 67.03% Ru, 60.61% Ru, 56.07% Ru, 56.07% Ru, 46.17% Ru, 37.92% Ru, 28.42% Ru, and Pure Pt (0% Ru).

RESULTS

Figure 1 shows x-ray diffraction data for the samples. The most visible and easy to index peaks are noted on the graph; the 100 and 101 HCP peaks on the Pure Ru sample data, and the 111 and 200 FCC peaks on the Pure Pt diffraction data. A determination of phase is garnered from the relative intensities of the peaks of the middle samples to the peaks of the pure samples. The samples in the middle, which have increasing percentages of Platinum as they move down the graph, show either FCC, HCP, or mixed phases. From visual analysis, 0% Ru through 46.17% Ru show a majority FCC structure; 56.07% Ru and 60.61% Ru are mixed phase; and from 67.03% Ru through 100% Ru, the samples demonstrate a HCP structure.

The FCC lattice parameters of samples that exhibited FCC structure were calculated using the formula $A = (2\pi / Q) \bullet \sqrt{h\text{^}2 + k\text{^}2 + l\text{^}2}$ where $Q = (4\pi \sin(\theta)) / \lambda$ where θ is the Bragg angle and λ is the wavelength of the incident beam [14]. These parameters were then plotted versus the percentage Ruthenium as shown in Figure 2.. These results were compared to the bulk results from Gurau and Gasteiger [2, 5]. In both cases, the lattice parameter decreases as the percentage Ruthenium increases; Ru atoms are replacing Pt atoms in the lattice and Ru (Z=44) is a much smaller atom than is Pt (Z=78). The thin film data show a different trend from the bulk as the percent Ruthenium approaches 40%; the concavity of the plot reverses.

Figure 3 is a graph of the areas under major FCC and HCP peaks versus percentage Ruthenium. The areas under major FCC peaks decrease and areas under major HCP peaks increase as the percentage of Ruthenium gets larger. From this, we

were able to produce a phase diagram. We chose ~ 35% Ru and ~60% Ruthenium as critical transition points, as these are spots were there is significant change in the areas under the peaks. Figure 4 is a comparison of our thin film phase diagram with the bulk phase diagram of Gasteiger [5], and is the major result of this study.

DISCUSSION AND CONCLUSION

Bulk RuPt has been well characterized, but prior to now, the accurate determination of crystalline structure of this bi-metallic alloy in thin-film form has not [9]. This may be important to those who seek to make the most efficient (performance-wise and financially-wise) thin-film anode catalysts for direct methanol fuel cells. The results of the analysis of the diffraction patterns allowed us to construct a phase diagram of thin film RuPt and compare it to the bulk RuPt diagram. Bulk data shows majority FCC from 0 – 62% Ru, mixed phase from 62 – 80%, and majority HCP from 80 – 100% [2, 5]. Our analysis shows that the co-sputtering method shifts that phase diagram to the left. The thin-film data shows majority FCC from 0 – 35%, mixed phase from 35 – 60%, and majority HCP from 60 – 100%. Also, lattice parameter changes proceed in a dissimilar fashion for thin films. With bulk RuPt, plotting lattice parameter versus percentage Ruthenium gives a nice, gently negatively sloping curve [5, Figure 2]. The thin-film data is much different; there seems to be a linear relationship for 0 – 30% Ruthenium, and then 30 – 60% manifests as an x^2 fit. The concavity is opposite for the thin-films from the bulk data [2, 5].

REFERENCES

[1] Kyung-Won Park, Jong-Ho Choi, Kwang-Soon Ahn, Yung-Eun Sung. "PtRu Alloy and Pt Ru-WO_3 Nanocomposite Electrodes for Methanol Electrooxidation Fabricated by Sputtering Deposition Method," Unpublished.

[2] Bogdan Gurau, Rameshkrishnan Viswanathan, Renxuan Liu, Todd J. Lafrenz, Kevin L. Ley, E.S. Smotkin, Erik Reddington, Anthony Sapienza, Benny C. Chan, Thomas E.

Mallouk, S. Sarangapani, "Structural and Electrochemical Characterization of Binary, Ternary, and Quaternary Platinum Alloy Catalysts for Methanol Electro-oxidation," J. Phys. Chem. B. Volume 102, 9997 – 10003, 1998.

[3] Renxuan Liu, Hakin Iddir, Qinbai Fan, Gouyan Hou, Aili Bo, Kevin L. Ley, E.S. Smotkin, Y.-E. Sung, H. Kim, S. Thomas, A. Wieckowski, "Potential Dependent Infrared Absorption Spectroscopy of Adsorbed CO and X-ray Photoelectron Spectroscopy of Arc-Melted Single-Phase Pt, PtRu, PtOs, PtRuOs, and Ru Electrodes," J. Phys. Chem. B. Volume 104, 3518 – 3531, 2000.

[4] Charles W. Hills, Michael S. Nasher, Anatoly I. Frenkel, John R. Shapley, and Ralph G. Nuzzo, "Carbon Support Effects on Bimetallic Pt-Ru Nanoparticles Formed from Molecular Precursors," Langmuir. Volume 15, 690-700, 1999.

[5] H. A. Gasteiger, P. N. Ross, Jr. and E. J. Cairns, "LEIS and AES on sputtered and annealed polycrystalline Pt-Ru bulk alloys," Surface Science. Volume 293, 67 – 80, 1993.

[6] Charles W. Hills, Nathan H. Mack, Ralph G. Nuzzo, "The Size-Dependent Structural Phase Behavior of Supported Bimetallic (Pt-Ru) Nanoparticles," J. Phys. Chem. B. Volume 107, 2626 – 2636, 2003.

[7] Cheng Pan, Fabrice Dassenoy, Marie-José Casanove, Karine Philippot, Catherine Amiens, Pierre Lacante, Alain Mosset, Bruno Chaudret, "A New Synthetic Method toward Bimetallic Ruthenium Platinum Nanoparticles; Composition Induced Structural Changes," J. Phys. Chem. B. Volume 103, 10098 – 10101, 1999.

[8] Kyung-Won Park, Jong-Ho Choi, Boo-Kil Kwon, Seol-Ah Lee, Yung-Eun Sung, Heung-Yong Ha, Seong-Ahn Hong, Hongsun Kim, Andrzej Wieckowski, "Chemical and Electronic Effects of Ni in Pt/Ni and Pt/Ru/Ni Alloy Nanoparticles in Methanol Electrooxidation," J. Phys. Chem. B. Volume 106, 1869 – 1877, 2002.

[9] Michael S. Nasher, Anatoly I. Frenkel, David L. Adler, John R. Shapley, Ralph G. Nuzzo, "Structural Characterization of Carbon-Supported Platinum-Ruthenium Nanoparticles from the Molecular Cluster Precursor $PtRu_5C(CO)_{16}$," J. Am. Chem. Soc. Volume 119, 7760 – 7771, 1997.

[10] Kyung-Won Park, Kwang-Soon Ahn, Jong-Ho Choi, Yoon-Chae Nah, Yung-Eun Sung, "PtRu-WO_3 nanostructured alloy electrode for use in thing-film fuel cells," Applied Physics Letters. Volume 82, Number 7. 1090 – 1092, 17 February 2003.

[11] Kyung-Won Park, Yung-Eun Sung, Michael F. Toney, "RuPt-WO_3 Alloy Thin-Film Nanostructures Grown by Co-sputtering Method," Unpublished.

[12] Hubert A. Gasteiger, Nenad Markovic, Philip N. Ross, Jr, Elton J. Cairns, "Methanol Electrooxidation on Well-Characterized Pt-Ru Alloys," J. Phys. Chem. Volume 97, 12020 – 12029, 1993.

[13] PJ Brucat, C*HM 2041 Lecture,* http://itl.chem.ufl.edu/2041_f97/lectures/lec_h.html, (July 2004).

[14] R. Nave, "Bragg's Law", *Hyperphysics*, http://hyperphysics.phy-astr.gsu.edu/hbase/quantum/bragg.html (July 2004).

[15] P.A. Christensen, "Introduction to Fuel Cells", *Direct Methanol Fuel Cell Research,* http://www.staff.ncl.ac.uk/p.a.christensen/dmfc1.htm (July 2004).

[16] *Direct Methanol Fuel Cells,* http://www.fctec.com/fctec_types_dmfc.asp (July 2004).

ACKNOWLEDGEMENTS

This experiment ran at beam lines 7-2 and 11-3 at the Synchrotron Radiation Laboratory at the Stanford Linear Accelerator Center from mid-July to early August. I'd like to thank the US Department of Energy for sponsoring the SULI program, my mentor, Michael Toney, for his guidance through this worthy project, Apurva Mehta, for our crash courses in X-ray diffraction, Roberto Vega for his patience, and all the other SULI students, for a good time.

Figure 1:

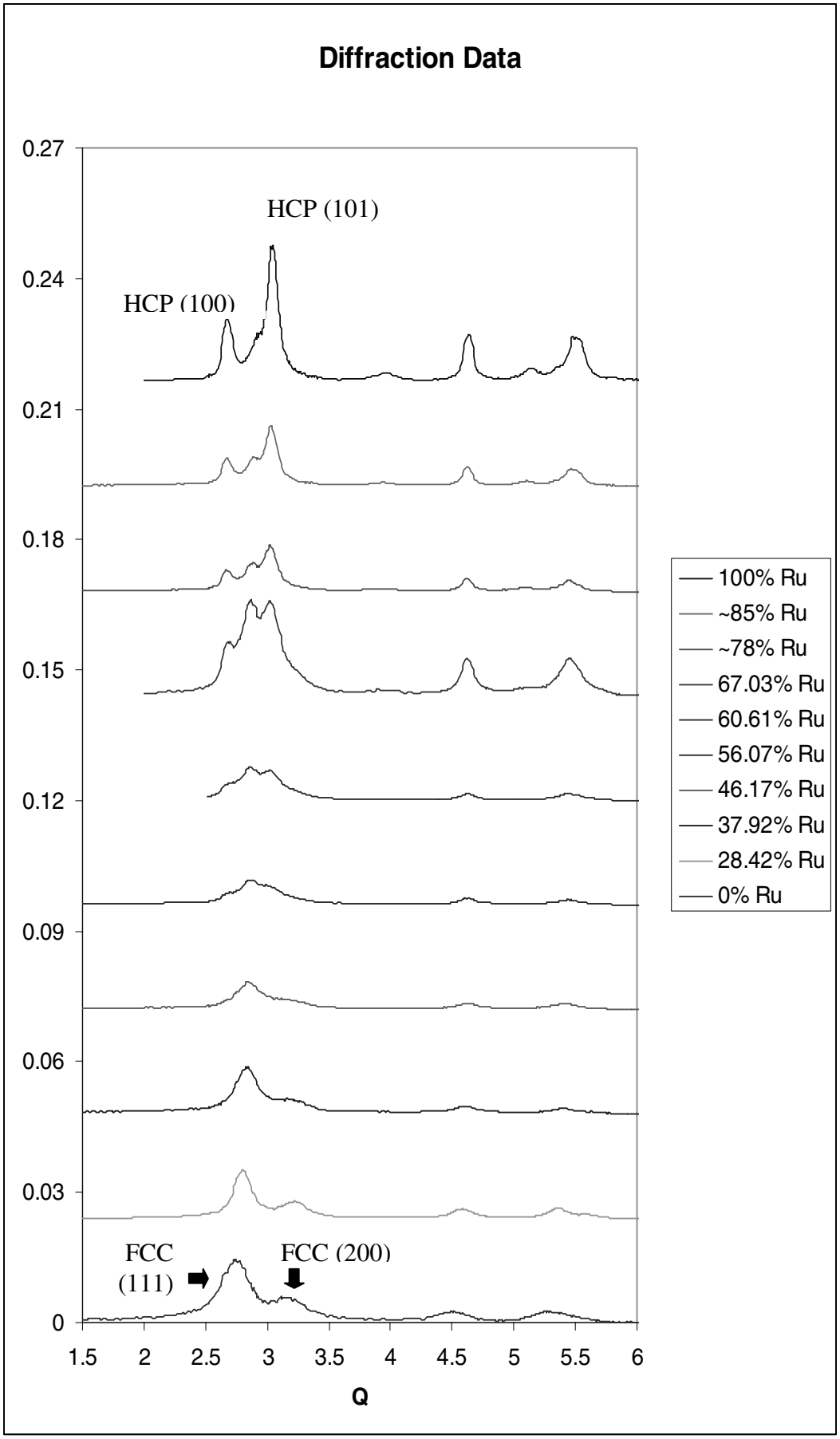
Diffraction Data
0.27
0.24
0.21
0.18
0.15
0.12
0.09
0.06
0.03
0
HCP (101)
HCP (100)
FCC (111)
FCC (200)
1.5
2
2.5
3
3.5
4
4.5
5
5.5
6
Q
100% Ru
~85% Ru
~78% Ru
67.03% Ru
60.61% Ru
56.07% Ru
46.17% Ru
37.92% Ru
28.42% Ru
0% Ru

Figure 2:

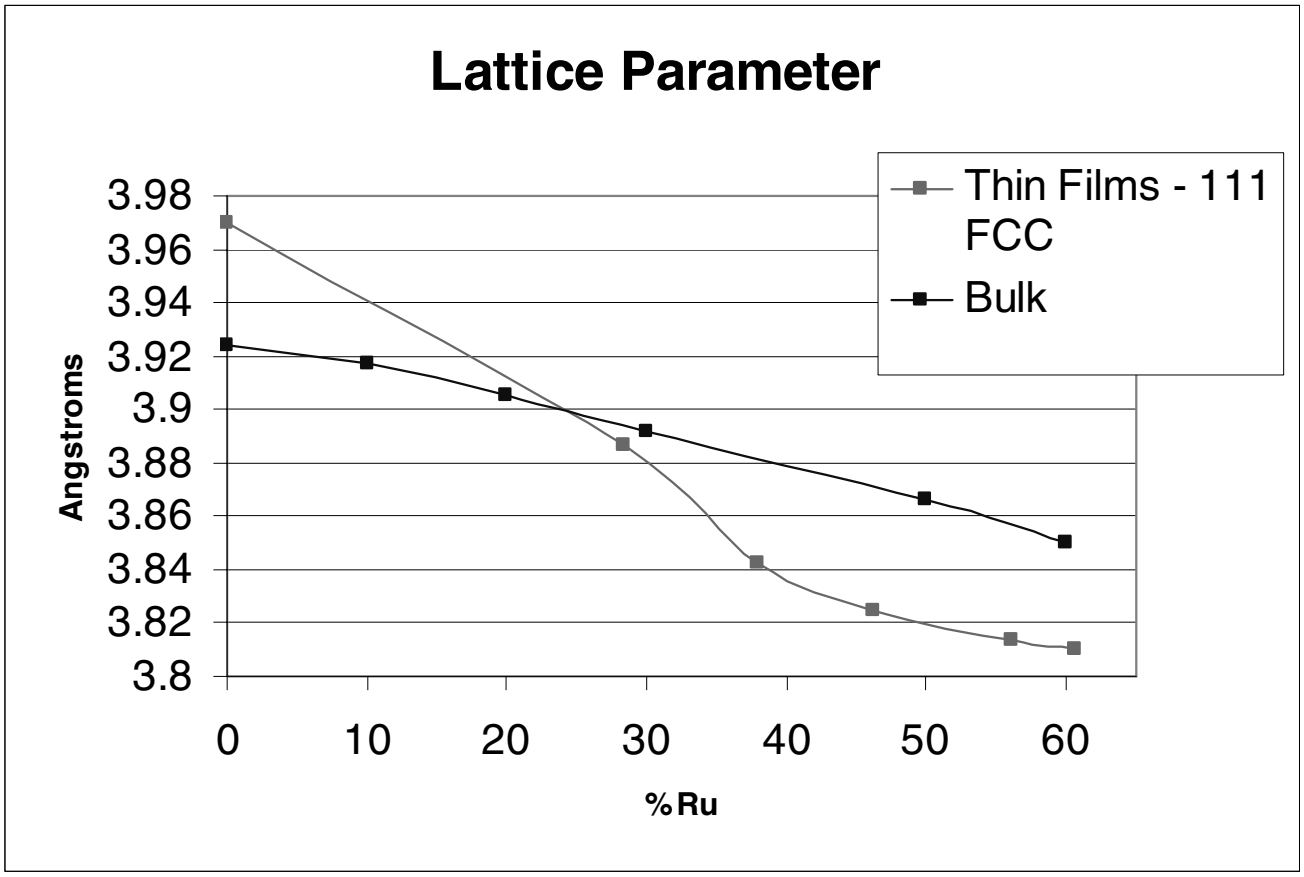

FCC lattice parameter measurements from diffraction data
using: $A = (2\pi / Q) \bullet \sqrt{h\text{^}2 + k\text{^}2 + l\text{^}2}$ where $Q = (4\pi \sin(\theta)) / \lambda$ where θ is the Bragg angle and λ is the wavelength of the incident beam

Figure 3:

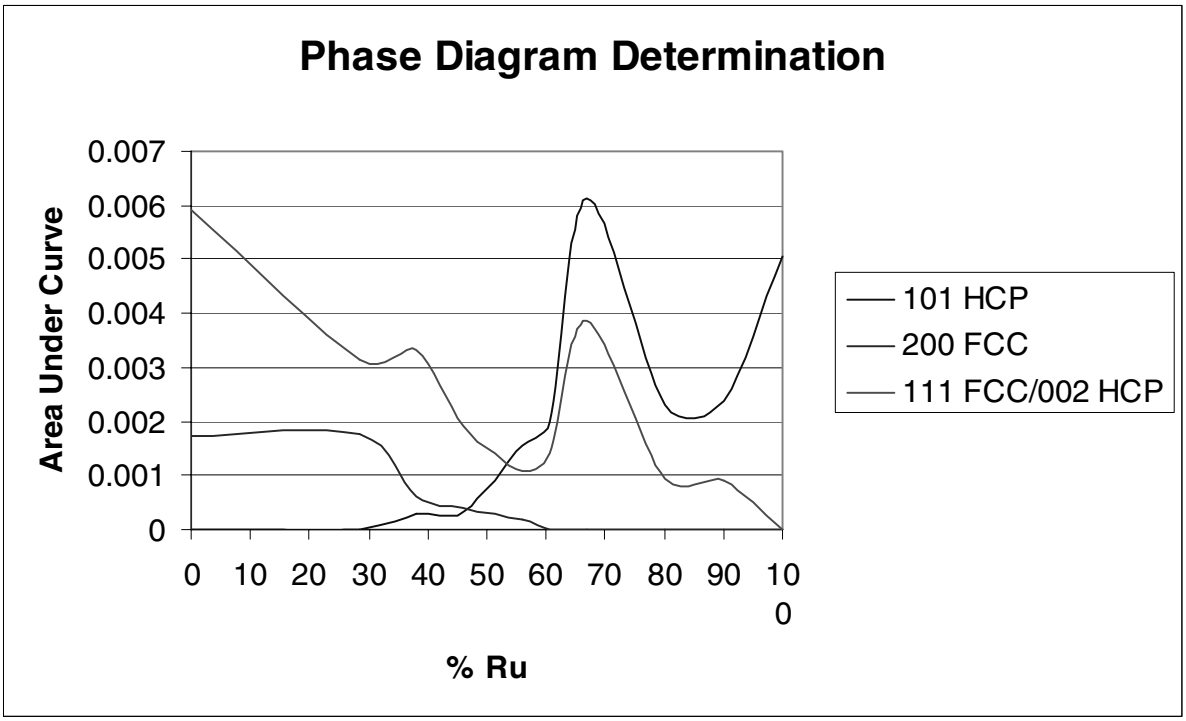

Areas under three major FCC and HCP curves versus percentage Ruthenium; used to determine RuPt thin film phase diagram.

Figure 4:

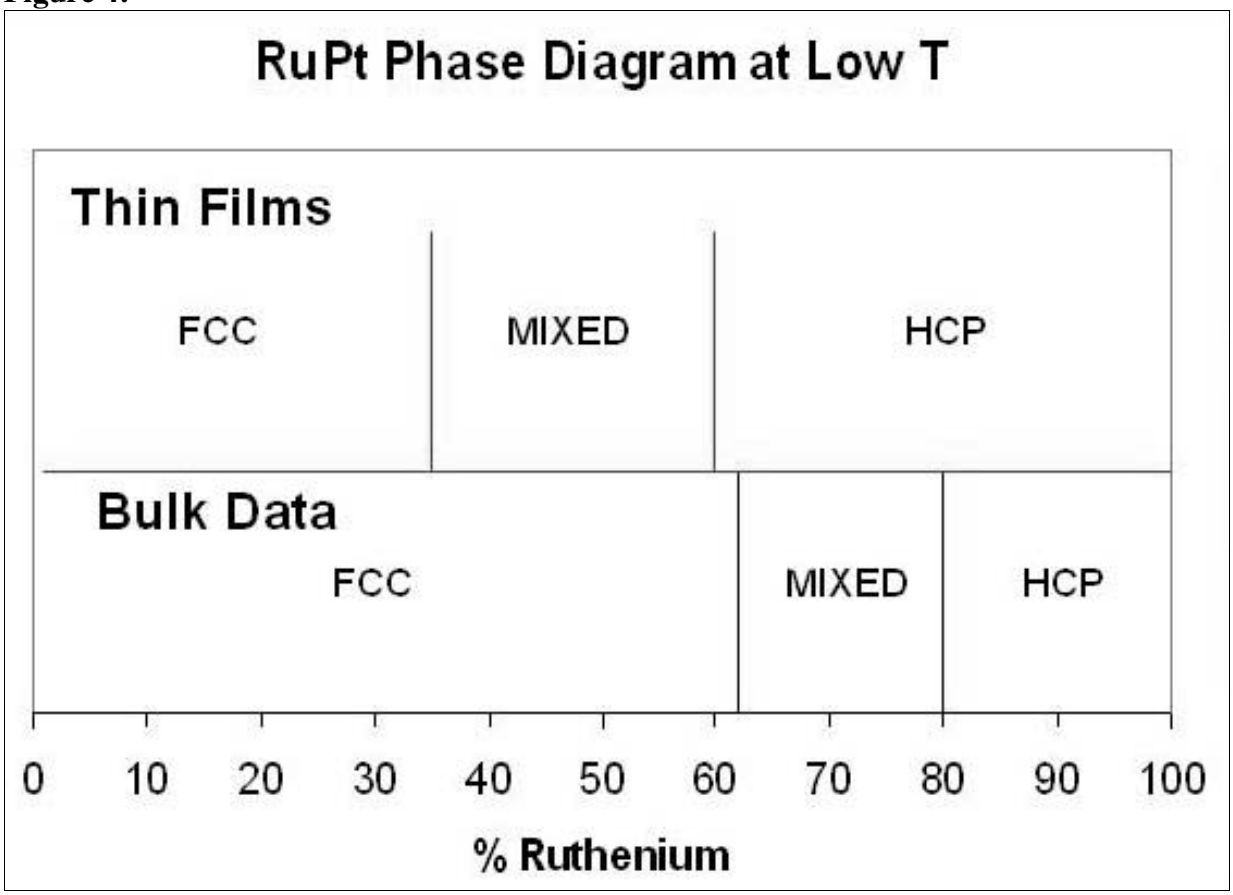

RuPt phase diagram constructed from the information in Figure 3 and from bulk data from Gasteiger [5]. The thin film phase diagram is shifted to the left, and has a wider mixed phase.